Proceedings of Symposium on Ultrasonic Electronics, Vol. 33 (2012) pp. 179-180
13-15 November, 2012

Analysis on Nonlinear Ultrasonic Images of Vertical Closed Cracks by Damped Double Node Model

減衰二重節点モデルを用いた閉じた縦き裂の非線形超音波映像の解析

Kentaro Jinno[1†], Masako Ikeuchi[2], Akihiro Ouchi[3] , Yoshikazu Ohara[1], and Kazushi Yamanaka[1]([1]School of Eng., Tohoku Univ.)
神納 健太郎[1†], 池内 雅子[2], 大内 彬寛[3], 小原 良和, 山中 一司([1]東北大 工)

1. Introduction

Evaluation of closed crack is most serious issue for safety of important structure such as power plants or air planes. To solve this problem, nonlinear ultrasound, in particular subhamonics [1] is promising, and we have developed a practical imaging method, subharmonic phased array for crack evaluation (SPACE [2]). However, one dimensional analysis (e.g. [1]) is not enough for practical design of testing equipment. So, we have reported 2D analysis of subharmonic generation at deep closed cracks using damped double nodes (DDN) by finite-difference time-domain (FDTD) method. In this report, we extend the DDN model to deal with not only lateral but also vertical cracks encountered in real conditions, and compare simulated results with experimental results

2. Concept of damped double node (DDN) model

In the previous DDN model, its crack face was parallel to the back face [3]. So, we extended lateral crack to vertical one which is similar to real condition.

In the open state, the normal nodes are split to double nodes consisting of the particle velocity of incidence-side crack face $\dot{u}^-$ and particle velocity of transmission-side crack face $\dot{u}^+$. To simulate closed crack faces with compression residual stress, we introduced a viscous damping [3].

(1) At the closed state, the tensile stress of the node at is calculated as the average of the stress of the left and right nodes of $x = i$ and $x = i - 1$, such that

$$T_{1M} = \frac{1}{2}\{{T_1}^n(i,j) + {T_1}^n(i-1,j)\}. \quad (1)$$

If $T_{1M} \leq T_{th}$, the nodes remain close and if $T_{1M} > T_{th}$, the nodes are opened, where T_{th} is the compression residual stress giving the threshold for transition.

(2) At the open state, the particle velocity nodes $\dot{u}^+$ and $\dot{u}^-$ have viscous damping proportional to the particle velocity difference between $\dot{u}^+$ and $\dot{u}^-$, so that

$$\dot{u}^{+n+1}(i,j) = \dot{u}^{+n}(i,j) + 2V_{PL}{T_1}^n(i,j) - \gamma\{\dot{u}^{+n}(i,j) - \dot{u}^n(i+1,j)\} \quad (2)$$

$$\dot{u}^{-n+1}(i,j) = \dot{u}^{-n}(i,j) + 2V_{PL}{T_1}^n(i-1,j) - \gamma\{\dot{u}^{-n}(i,j) - \dot{u}^n(i-1,j)\} \quad (3)$$

where γ is the damping coefficient, and V_{PL} is the normalized longitudinal wave velocity. Displacements are given by calculating as an integral of particle velocity $\dot{u}^+$ and $\dot{u}^-$, respectively. The crack opening displacement (COD) is given as

$$\Delta u^n = u^{+n} - u^{-n} \quad (4).$$

If $\Delta u > 0$, the crack remain open, and if $\Delta u \leq 0$, the crack is closed.

3. Analisis

3-1. Simulation condition

Calculation was carried out with a time interval of 1.727 ns and node interval of 0.02 mm in model of **Fig. 1**. Simulating SUS316L used for nuclear power plants, stffiness tensile components were set up C_{11}＝277 GPa and C_{12}=82 GPa.

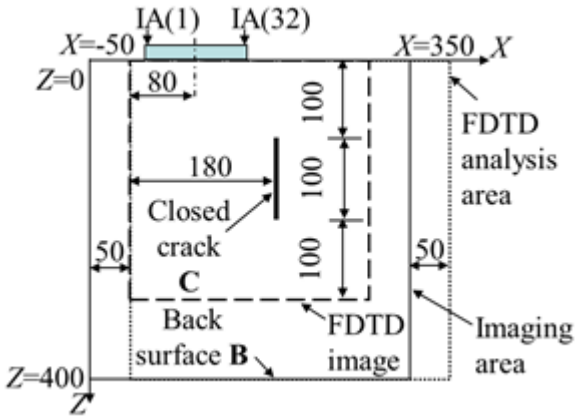

Fig. 1 Simulation model with a phased array

Plane waves of 3 cycle burst at frequency f =8 MHz was excited by a 32-element array at the surface, with the incidence wave amplitudes at the crack surface of 40 nm and 160 nm. Residual compression stress was set to 100 MPa. The damping coefficient was set to 0.7 to suppress the noise.

3-2. FDTD image

With 40 nm amplitude, there is no response. Fig. 2 shows FDTD image with 160 nm amplitude, there are scattered waves at the crack. This example represents the fact that closed cracks are opened by a large amplitude wave. And, scattered wave (b) and (c) generated at each crack tips are observed.

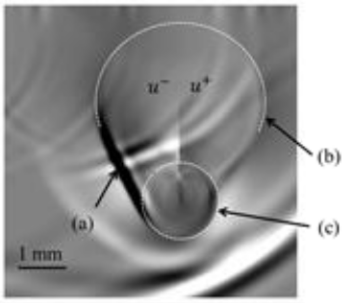

Fig. 2 FDTD image of scattered waves

3-3. FA and SA images

By using SPACE [2] algorithm, we calculated fundamental array (FA) and subharmonic array (SA) images. FA image is calculated by filtering between 6~10 MHz, and SA image is calculated by filtering 2~7 MHz. With 40 nm amplitude, closed crack is not imaged.

FA and SA images with 160 nm are shown in Fig. 3. In SA image, crack responses from its top and bottom are visualized. Back surface is appeared in SA image. It is an artifact due to the leak of frequency [4]. On the other hand, crack responses are appeared in FA image. This is the phenomenon that fundamental frequency generates with large amplitude incidence.

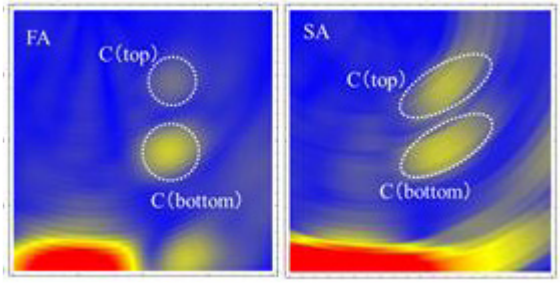

Fig. 3 FA and SA images

3-4. Analysis of crack top and bottom

Sift averaged wave forms at crack top (180,100) and bottom (180,200) which are visualized in FA and SA images are shown in Fig. 4. And, each wave forms are analyzed with wavelet transform.

In (b), frequency peak surrounded by white circle at 4 MHz (f/2) is observed more clearly than in (a).

Studying this phenomenon in more detail enables us to optimize closed crack detection condition.

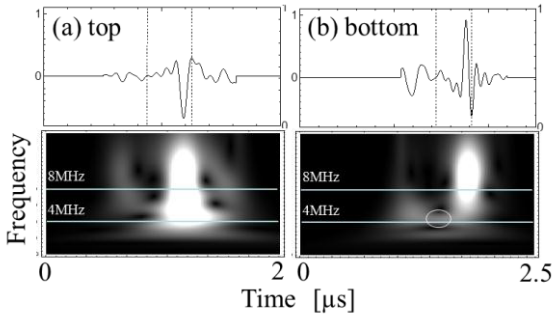

Fig. 4 Shift averaged wave forms and wavelet transform at crack top (a) and bottom (b)

3-5. Comparison with experimental result

Fig. 5 shows SA image of previous experimental result of SUS316L fatigue specimen [2]. In this experiment, incident frequency was 7 MHz.

In SA image, crack top A and middle point B were observed. Thus, the simulated SA image using the vertical crack model (Fig. 3) reproduces the feature of multiple scattering points within a single crack, observed in the experiment.

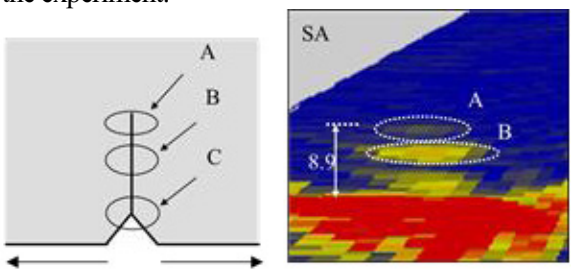

Fig. 5 Experimental result of fatigue specimen

4. Conclusion

Vertical closed cracks by damped double node model (DDN) [3] can reproduce the SA image of the previous experimental result of closed crack. Therefore, this model can reproduce real experiments. Hereafter, we will study optimum conditions for subharmonic generation, and this model is expected to help us comprehend its phenomenon.

References

1. K. Yamanaka, T. Mihara, T. Tsuji, Jpn. J. Appl. Phy., 43 (2004) 3082.
2. Y. Ohara, T. Mihara, R. Sasaki, S. Yamamoto, K. Yamanaka, Appl, Phys. Lett., 90 (2007) 011902
3. K. Yamanaka, Y. Ohara, M. Oguma, Y. Shinkaku, APEX., 4 (2011) ,076601-1-3
4. Y. Ohara, S. Horinouchi, M. Hashimoto, Y. Shintaku, K. Yamanaka: Ultrasonics, 51 (2011) 661.